Volume 9, Issue 6, 2019, 4567 - 4574 ISSN 2069-5837

Biointerface Research in Applied Chemistry

www.BiointerfaceResearch.com

https://doi.org/10.33263/BRIAC96.567574

Original Research Article **Open Access Journal**

Received: 03.09.2019 / Revised: 20.10.2019 / Accepted: 22.10.2019 / Published on-line: 26.10.2019

Green synthesis approach and theoretical studies for Cr(III), Mn(II), Fe(III), Co(II) and Ni(II) complexes with NNS donor Schiff base ligand

Tarek Ahmed Yousef [1, 2, *]

[1]Department of Chemistry, Science College, Imam Mohammad Ibn Saud Islamic University, (IMSIU), Riyadh, KSA, P.O. Box 90950, Riyadh 11623,Saudi Arabia
[2]Department of Toxic and Narcotic drug, Forensic Medicine, Mansoura Laboratory, Medicolegal organization, Ministry of Justice, Egypt
*corresponding author e-mail address: ***TAYousef@imamu.edu.sa*** | Scopus ID 36562771600

ABSTRACT

The green synthetic processes have synthetized five Cr(III), Mn(II), Fe(III), Co(III) and Ni(II) complexes. In the current study, their synthesis by ball mining is decorated in a simple one-pot synthesis, cost efficiency, easy to measure for commercial manufacture, effective synthesis conditions such as moderate temperature and shorter length, thus preventing further by-products which could cause environmental harm, and being environmentally friendly as it is. All five complexes are well-defined, polyncrystalline materials as their Powder X-ray diffraction patterns indicate. The characterization of these complexes had been Fourier Transform Infrared Spectroscopy(FT-IR), ^1H-^{13}C Nuclear magnetic resonance, Scanning Electron Microscopy (SEM), electronic absorption spectral studies as well as magnetic studies and Powder XRD techniques.

Keywords: *Thiosemicarbazone complexes; Thermal analysis; Scanning Electron Microscopy; Powder XRD ; molecular modelling.*

1. INTRODUCTION

Ball milling is a mechanical procedure broadly utilized for grinding to acquire powders with fine particles [1-4]. In traditional strategies, reactants are broken apart by solvent molecules. Thiosemicarbazones and semicarbazones have a great ability to complex with transition metals. They are also very biologically active and many studies show that complexation can influence their biological activity. The molecules comprising the C = N double bond in the RC = N-R 'sequence have been extensively studied because of the numerous properties of this functional unit both in terms of acid-base properties and oxido-reductive properties, and even photochemical properties [5]. Thiosemicarbazones, semicarbazones and their derivatives are the main subgroups of hydrazones (-C=N-N-), in addition to thioaroylhydrazones and oxyaroylhydrazones. These are compounds that are usually obtained by the condensation of a ketone or an aldehyde with thiosemicarbazide, semicarbazide [6]. The existence of different donor atoms in these molecules ensures the stability of their complexes: mainly the nitrogen atom of the imine function and that of sulfur of the thioamide function (thiosemicarbazone) and the carbonyl oxygen atom (semicarbazone) as well as other donor atoms from the heterocycle carrying the function or another functional group. Like thiosemicarbazones, semicarbazones (RR'C =N-NH-C(O)-NH_2) also have the ability to complex with various metal ions. However, semicarbazones are less complex than thiosemicarbazones [7]. Sulfur and nitrogen donors would coordinate the metal center to form bident, trident and even polyvalent ligands and thereby create complexes of distinct geometry and characteristics to change or improve their biological characteristics. [8, 9]. In the literature, semicarbazones have been generally less studied than thiosemicarbazones. They are also biologically active and many studies show that this activity can increase with complexation [10, 11]. We continued in the past reporting [12] on the coordinating behavior of HL with the spectroscopic and computational methods of Cr(III), Mn(II), Fe(III), Co(II) and Ni(II) ions.

2. MATERIALS AND METHODS

2.1. Material.

All solvents and reagents used were of the reagent / molecular biology grade and were used for commercial purposes. For spectral measurement, spectroscopic solvents were utilized while metal salts from sigma Aldrich were bought and used as received.

2.2. Synthesis of ligand and their metal complexes.

2.2.1. Synthesis of ligand.

2.2.1.1. (Z)-2-(4-(dimethylamino)benzylidene)hydrazine-1-carbothioamide. Thiosemicarbazide (9.5 g and 10 mmol) and p-diaminobenzaldehyde (15 g, 10 mmol) in 1: 1 molar ratio were heated for 2 to 4 hours under reflux. The solids were filtered, dried and recrystalled after cooling.

2.2.2. Synthesis of metal complexes complexes.

All complexes were prepared using refluxing (1 mmol ligand + 1 mmol metal salt) ($MnCl_2.4H_2O$, $NiCl_2.6H_2O$, $CrCl_3.6H_2O$, $FeCl_3$, and $CoCl_2.6H_2O$ in an ethanol solution for 2-3 hours. The solid formed complex washed off with absolute ethanol, followed by diethylether to remove any unreacted metal and finally dried in the vacuum desiccator, over an absolute ethanol and a vacuity deicer. The compounds have been filtered off and then dried in an ethanol-free solution for duration of 2-3 hours.

2.3. Molecular modeling.

The attempt has been made with the hyperchem program strengthfield series introduced in hyperchem 8 [13] to obtain a better understanding of the molecular structure of the ligand and its complexes, geometric optimization and conformation analysis

[14]. The method of molecular mechanics has been used to quickly explore the geometries of the proposed metal complex structures. In the case of AM1 and PM3 (Polak–Ribiere) RMS 0.01 kcal, the lowly lying conformers achieved from this search were then optimized.

2.4. Analyses of the complexes.

2.4.1. Elemental analyses.

The Perkin – Elmer 2400 Series II Analyzer was used for elementary analyses (C, H and N). A conventional technique was employed to analyze the metal content and halide in complex.

2.4.2. Physico-chemical measurements.

The SPEX 8000 mixer with stainless steel vials of 10 cm^3 was used in the ball mill in this research. Melting points have been deterred by a Stuart melting point device SMP10. Perkin – Elmer's FTIR spectrometer 2000 registered infrared spectra as KBr pellets in the spectral range 4000–400 cm^{-1}. JEOL NMR ECA-500MHz was achieved with a 5 mm D_2O-DMSO sample head for ^1H and 13C NMR room temperature measurement. On a Unicam UV – Vis spectrophotometer UV2, in the range of 200–900 nm, the ligand spectra and its metal complexes were recorded in DMSO solution. A Johnson Matthey magnetic susceptibility balance with a calibratant use of $Hg[Co(SCN)_4]$ was used as a measuring magnet at room temperature (25 + 1°C). Using CU-Kα radiation at 40 kV and 40 mA, POUDDER XRD (PAN analysis X'Pert PRO, Boulder, CO, USA) was performed. The scans were typically performed over a2θ range of 10 to 80 at a speed of 0.02/s. The morphology of the powder was examined by SEM (JSM-6380LA, JEOL -Japan Electron Optics Laboratory, Tokyo, Japan).

3. RESULTS

We seek to specify some structural elements in order to be able to make structural propositions for all the compounds that did not give single crystals, by using the data obtained by the spectroscopic techniques such as the study of the infrared spectra and the study of the ^1H NMR proton nuclear magnetic resonance. The complexes prepared are non-hygroscopic, water-insoluble and most organic soluble but can be dissolved in DMF or DMSO. We cannot isolate the appropriate crystals for X-ray measurements. All the solid complexes have been isolated in a pure state. The compositions of the isolated complexes are agreed with the proposed formulae and found data listed in (Table 1). The color of the most thiosemicarbazone complexes is intense and that may be due to sulfur to metal charge transfer in addition to d-d transitions, which dominates their visible spectra [15].

3.1. Spectral studies.

3.1.1. ^1H - ^{13}C NMR spectra.

The ^{1}HNMR spectrum of HL in DMSO-d_6 (Fig.1) was recorded and showed signals at: δ 1.222 ppm (4H, s, two CH_2), δ 2.948 ppm (6H, s, two CH_3), δ 6.695 ppm (2H, s, NH_2-CS), δ 11.149 ppm (1H, s, N-NH-CS), δ 7.973 ppm (1H, s, Ph-CH-C), δ 7.735 (2H, Ph, d), δ 7.557 ppm (2H, Ph, d).
The NH protons peaks vanished with D_2O, which means they can be replaced readily.

The important characteristics have been identified in the ^{13}C NMR spectrum of HL (Fig. 2) were detected; it shows signals at: (39.083, 39.123) ppm for two CH3, (42.083, 42.123) ppm for two CH_2, (111.653) ppm for C2, C4, (121.395) ppm for C6, (128.567) ppm for C1, C5, (143.286) ppm for C3, (151.360) ppm for C10 and (177.935) ppm.

3.1.2. Infrared spectra.

The commitment of an organic molecule as a ligand in a metal complex is accompanied by modifications of its infrared spectrum. These modifications are represented by: - Moves of bands - The appearance of new bands - The disappearance of some bands - The multiplication of some bands
In Table 2 are registered the principal infrared bands of HL and its metal complexes.

The ligand (HL) IR spectrum shows bands with values of 3365 and 3243 cm^{-1} assigned to each group of $\nu(NH_2)$ and ν(NH) respectively. The bands appeared at 812 cm^{-1} is due to ν(C=S) while the band at 1585 cm^{-1} is assigned to $\nu(C=N)^a$ group.

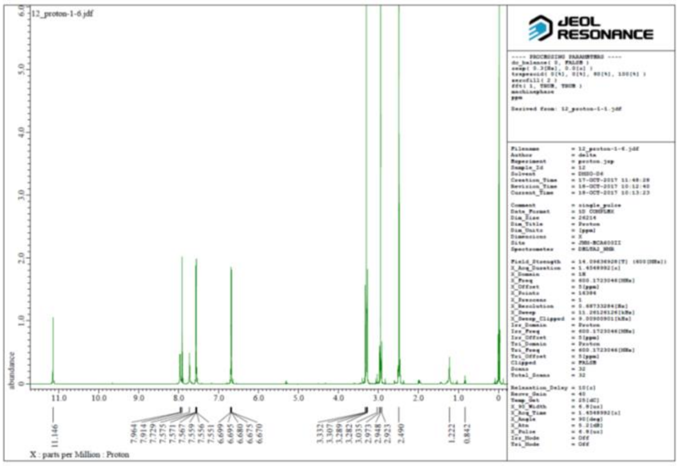

Figure 1. ^1H NMR specrum of HL.

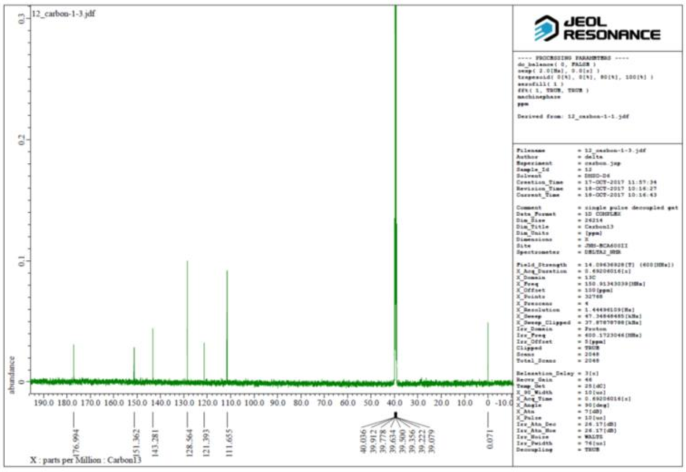

Figure 2. ^{13}C NMR spectrum of HL.

The ν (S-H) band generally around 2570 cm^{-1} is absent from the IR spectrum of the ligand. In contrast, the ν (NH) band is present at 3243 cm^{-1}. So in the solid state the ligand is in thione form. This is confirmed by the presence of the valence vibration band of the carbon-sulfur double bond at 1165 and 812 [16,17]. A thione/thiol tautomerism (HN-C = S / N = C-SH) in the solid state is excluded because there is no band of the ligand spectrum that is characteristic for the ligand of thiol at (2500-2650 cm^{-1}) [18].

A comparison of the IR spectra of HL and its metal complexes (Table 2) demonstrates that HL behaves in a neutral bidentate or mononegative bidentate manner according to the metal salt used.

In [$CrHLCl_3(H_2O)$], [$CoHLCl_2(H_2O)_2$] and [$NiHLCl_2(H_2O)_2$] complexes, The free or complex ligand is always thione form because the ν(C=S) band is present in both the ligand and complex spectra. Moreover, the presence of the ν(NH) band shows that the ligand is not deprotonated in the complexes. By comparing the spectrum of the ligand with those of the complexes, we find that the bands ν(C=S), ν(C=N) in the complexes are considerably displaced (between 11 and 58 cm^{-1}) with respect to their location in the ligand spectrum [19,20].

The absence of ν(NH) and ν(C=S) bands with simultaneous appearance of new bands in [$MnLCl(H_2O)_3$] and [$FeLCl_2(H_2O)_2$] complexes is due to ν(S-C=N) and ν(C-S) vibrations supports the deprotonation of SH group and the participating in coordination in the thiol form.

The ν(C=N)(azomethine) vibration shifts to lower wavenumber in [$MnLCl(H_2O)_3$] and [$FeLCl_2(H_2O)_2$] complexes or to higher wavenumber in [$CrHLCl_3(H_2O)$], [$CoHLCl_2(H_2O)_2$] and [$NiHLCl_2(H_2O)_2$] complexes indicating that this group participates in chelation [21,22].

As a consequence of a group of azomethines in coordination, the vibration ν(N-N) shifts into lower wavenumber in all complexes.

Table 1. Analytical and physical data of HL and its metal complexes.

Compound, Emperical formula, (F.Wt)	Color	M.P. (°C)	% Found (Calcd.)					Yield %
			C	H	N	M	Cl	
HL (12) $C_{10}H_{14}N_4S$ (222.31)	Yellow	220	53.78 (54.03)	6.48 (6.35)	24.98 (25.20)	-	-	85
[$CrHLCl_3(H_2O)$] (2) $C_{10}H_{16}Cl_3CrN_4OS$ (378.67)	Green	>300	30.38 (30.13)	3.89 (4.05)	14.59 (14.05)	13.55 (13.04)	26.23 (26.68)	78
[$MnLCl(H_2O)_3$] (3) $C_{10}H_{19}ClMnN_4O_3S$ (365.74)	Dark Yellow	>300	32.10 (32.84)	5.11 (5.24)	15.18 (15.32)	14.98 (15.02)	9.55 (9.69)	76
[$FeLCl_2(H_2O)_2$] (4) $C_{10}H_{17}Cl_2FeN_4O_2S$ (384.08)	Brown	>300	31.19 (31.27)	4.21 (4.46)	14.77 (14.59)	14.73 (14.54)	18.62 (18.46)	73
[$CoHLCl_2(H_2O)_2$] (5) $C_{10}H_{18}Cl_2CoN_4O_2S$ (388.17)	Dark Green	>300	30.78 (30.94)	4.55 (4.67)	14.61 (14.43)	15.39 (15.18)	18.39 (18.27)	80
[$NiHLCl_2(H_2O)_2$] (6) $C_{10}H_{18}Cl_2NiN_4O_2S$ (387.87)	Brown	>300	30.57 (30.96)	4.49 (4.68)	14.65 (14.44)	15.42 (15.13)	18.17 (18.28)	82

Table 2. Principle infrared bands of HL and its metal complexes.

Compound	ν(C=N)[a]	ν(C=S)	ν(NH_2)	ν(N-N)	ν(NH)	ν(C-S)
HL	1585	812	3365	933	3243	-
[$CrHLCl_3(H_2O)$]	1595	801	3370	943	3244	-
[$MnLCl(H_2O)_3$]	1538	-	3390	970	-	620
[$FeLCl_2(H_2O)_2$]	1572	-	3395	963	-	625
[$CoHLCl_2(H_2O)_2$]	1593	803	3373	941	3242	-
[$NiHLCl_2(H_2O)_2$]	1598	802	3372	940	3245	-

a: azomethine

3.2. Electronic Spectra and magnetic measurements.

In the dimethylsulfoxide (DMSO) solution and Nujol mull, electronic spectra were presented for all the complexes examined. The speculative assignments of the important electronic spectral absorption bands of HL metal complexes and magnetic moments are given in (Table 3).

The electronic spectra of [$CrHLCl_3(H_2O)$] shows two strong absorption bands at 17778 (ν_1) and 20841 (ν_2) cm^{-1}characteristic for octahedral Cr(III) complexes [23]. The ν_3 band was hidden below the CT band so we could not observe it. The following are three spin- allowed transitions in an octahedral field for Cr(III): $^4A_{2g}(F)\rightarrow{}^4T_{2g}(F)(\nu_1)$, $^4A_{2g}(F)\rightarrow{}^4T_{1g}(F)(\nu_2)$ and $^4A_{2g}(F)\rightarrow{}^4T_{1g}(P)(\nu_3)$. The transition of ν_1 is a direct ligand field parameter measurement 10 Dq. From ν_1 and ν_2, the value of B and β may be calculated. The μeff value 3.78 B.M can also be taken for the octahedral geometry as further proof.

The spectrum in the visible region is not different from that in the DMF solution with two bands of [$CoHLCl_2(H_2O)_2$] complex in the solid state. At 18251 cm^{-1}, the former is very large and dissymmetric, and at 192,335 cm^{-1}, the latter is very small and less intense. These bands are in good agreement for octahedral Co (II) complex [17]. According to the energy level diagram for high-spin octahedral Co(II) complexes, the first band is allocated to $^4T_{1g}(F) \rightarrow {}^4T_{1g}(P)$ and $^4T_{1g}(F) \rightarrow {}^4A_{2g}(F)$ transitions [24] arising from the high-spin d^7 configuration Co(II) in an octahedral geometry.

The electronic spectrum of [$NiHLCl_2(H_2O)_2$] complex exhibited two bands in the 17106 cm^{-1} for the first and at 21830 cm^1 regions for the second assignable to the $^{3}A_{2g}\rightarrow{}^{3}T_{1g}(F)(\nu_{2})$ and $^{3}A_{2g}\rightarrow{}^{4}T_{1g}(P)(\nu_{3})$ transitions, respectively characteristic for Ni(II) octahedral complexes [25].

The electronic spectra of $[MnLCl(H_2O)_3]$ complex show a band at 16933 and 23695 cm^{-1} respectively assigned to the $^{6}A_{1g}\rightarrow{}^{4}T_{1g}$ transition. The value of μ_{eff} (5.89 B.M.) is expected for a high spin $3d^5$ system and additional support for the proposed octahedral structures [26].

The μ_{eff} = (5.98 B.M) of $[FeLCl_2(H_2O)_2]$ complex, shows high spin octahedral geometry of d^5system. The values observed electronic transition bands at (22980 and 26778 cm^{-1}) and the values of ligand field parameters is good evidence that HL strongly coordinated and more covalent nature with Fe(III) ions.

3.3. Molecular modeling.

Density functional theory (DFT) is a computational quantum mechanical modeling method used to simulate the molecular conformation of isolated compounds (Structures 1-6). In addition, the quantum chemical parameters of organic as well as inorganic compounds assessed like E_{LUMO}, E_{HOMO}, dipole moment, binding energy and total energy (Table 4).

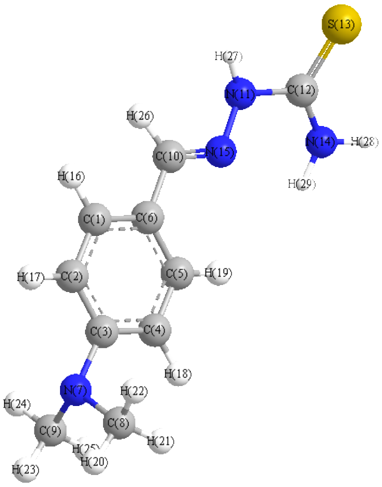

Structure 1. Optimized molecular structure of HL.

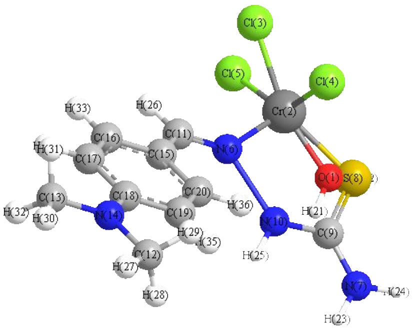

Structure 2. Optimized molecular structure of $[CrHLCl_3(H_2O)]$.

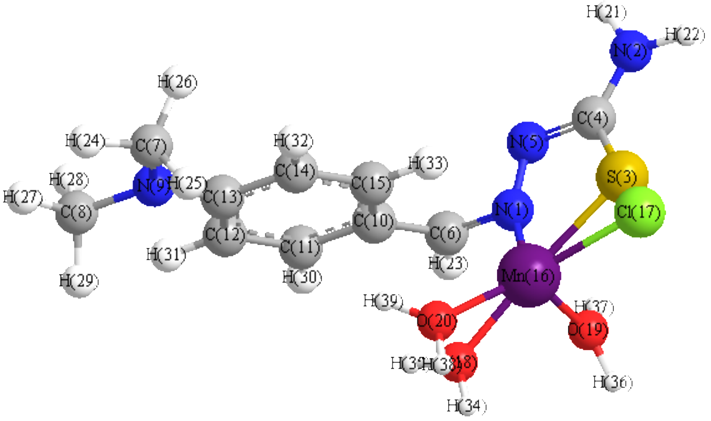

Structure 3. Optimized molecular structure of $[MnLCl(H_2O)_3]$.

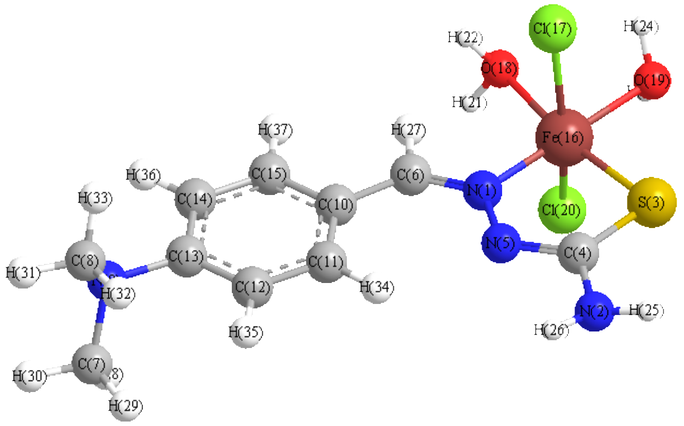

Structure 4. Optimized molecular structure of $[FeLCl_2(H_2O)_2]$.

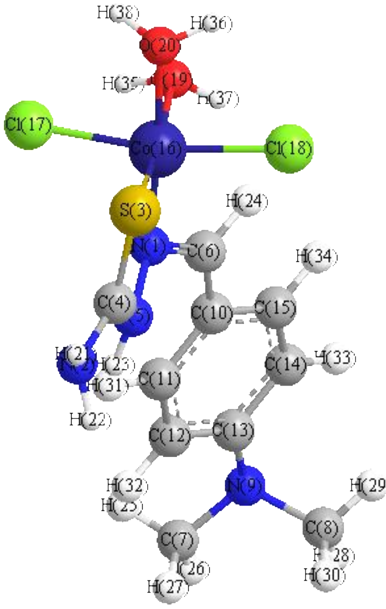

Structure 5. Optimized molecular structure of $[CoHLCl_2(H_2O)_2]$.

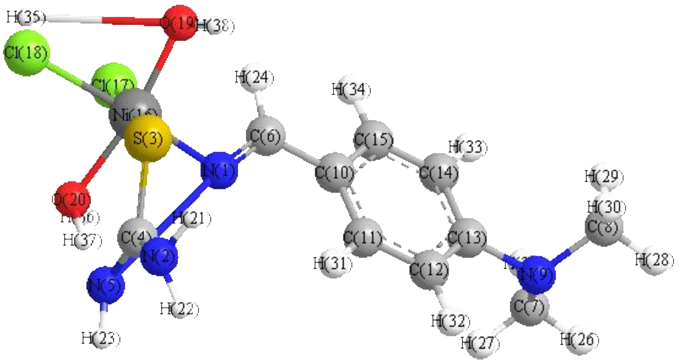

Structure 6. Optimized molecular structure of $[NiHLCl_2(H_2O)_2]$.

The results indicated that:

1- The energy gap (E_{HOMO} -E_{LUMO}) is considered as an essential steadiness list which portrays the kinetic stability and chemical reactivity of the molecule. This gap is used to build up a hypothetical model to clarify the concoction structure and affirms boundaries in a few atomic frameworks, which impacts the organic movement of the molecule. A molecule with a small gap is more polarized and is known as a soft molecule. It is realized that; soft molecules are more dynamic than the hard ones since they can offer electrons effortlessly to an acceptor. The energy gap is little in ligand showing that charge move effectively happens in it, which impacts the biological activity of the molecule. The Low energy gap is likewise ascribed to the groups that go into. LUMO and HOMO negative values were representing the stability of complexes [27-29].

2- The theory of FMOs also guesses the locations where aromatic compounds are coordinated (electrophilic attack). Initially, the response occurs with the highest overlap of the HOMO on one molecule and the LUMO on the other. A key factor in many reactions is the overlap between the HOMO and LUMO. The objective of the calculations is to find the highest molecular orbital coefficient values. Ligand orbits with the highest molecular orbital coefficients can, therefore, be regarded the coordinating sites. The calculation's results confirm that the nitrogen of the C = N group has the highest molecular-orbital coefficient values. The information shows this conclusion.

3- The higher values of the binding energy for isolated solid complexes than free ligand indicated the greater stability of the complexes than ligand alone.

4- The electrical charges separation in a system predictable by electric dipole moment, where the complexes have shown a greater dipole than free ligand, which improves the power of the isolated solid complexes [30].

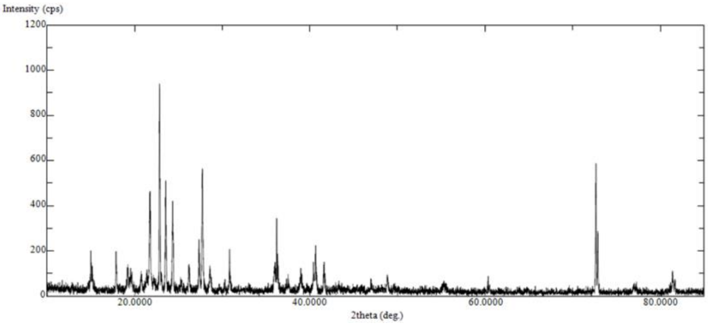

Figure 3. XRD patterns of HL.

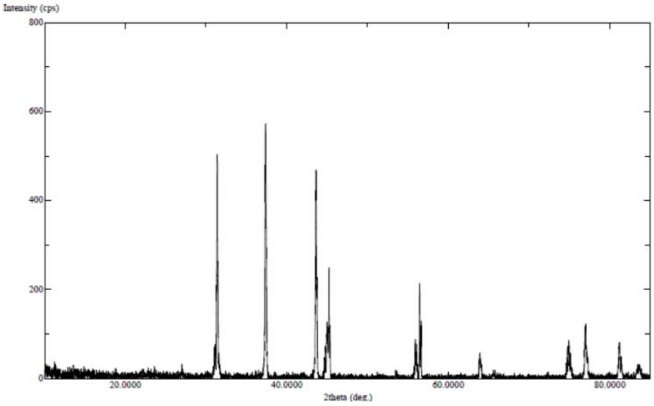

Figure 4. XRD patterns of [$CrHLCl_3(H_2O)$].

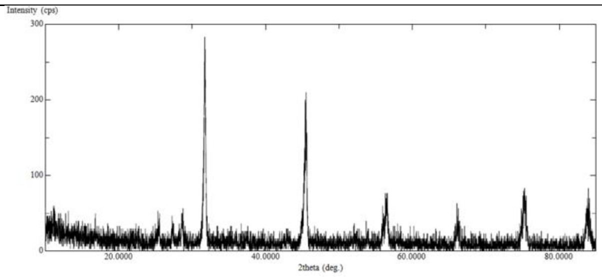

Figure 5. XRD patterns of [$MnLCl(H_2O)_3$].

Figure 6. SEM image of HL.

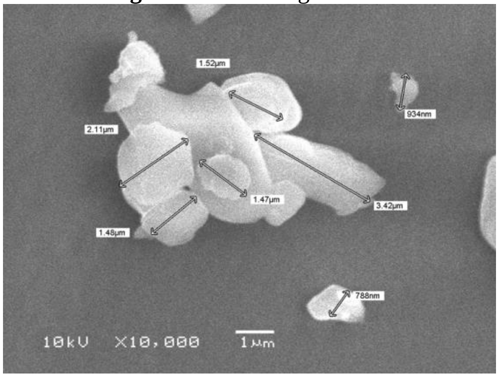

Figure 7. SEM image of [$CrHLCl_3(H_2O)$].

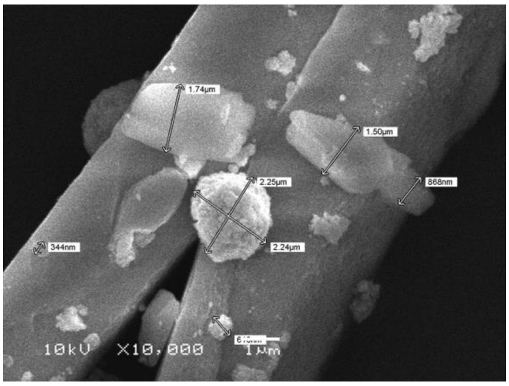

Figure 8. SEM image of [$MnLCl(H_2O)_3$].

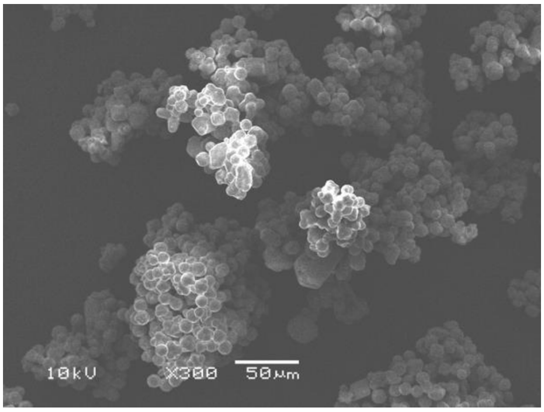

Figure 9. SEM image of [$FeLCl_2(H_2O)_2$].

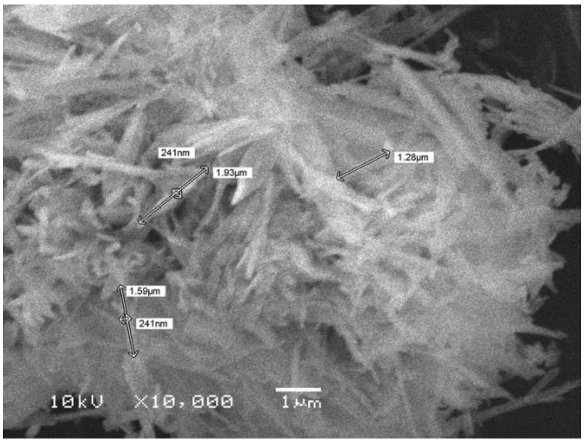

Figure 10. SEM image of [$CoHLCl_2(H_2O)_2$].

3.4. XRD Analysis.

XRD was carried out to identify the polycrystalline or amorphous nature of the synthesized samples. Powder XRD pattern of HL and complexes 1–6 were recorded over the 2θ (scattering angle) = 10–85° range. The spectra of ligand and its metal complexes displayed sharp crystalline peaks denoting their nano-crystallinity (Fig. 3). The dominant XRD peak at 27.74° 2θ was observed for HL, while the peaks for Cr(III), Mn(II), Fe(III), Co(II) and Ni(II) complexes were observed at 37.36°, 31.77°, 45.05°, 32.00° and 31.22 2θ, respectively. Therefore, the structural phase changes occurred with the chelation of Cr(III) (Fig. 4), Mn(II) (Fig. 5), Fe(III), Co(II) and Ni(II) with HL, which was apparent by the shift in the dominant 2θ value to the higher energy side. So far, the literature has not revealed the structural features of HL and its complexes Cr(III), Mn(II), Fe(III), Co(II) and Ni(II). Therefore the crystal structure of HL is being determined by crystal growth studies with the aim of a better knowledge of structural characteristics, including Cr(III), Mn(III), Fe(III), Co(II) and Ni(II) complexes [31].

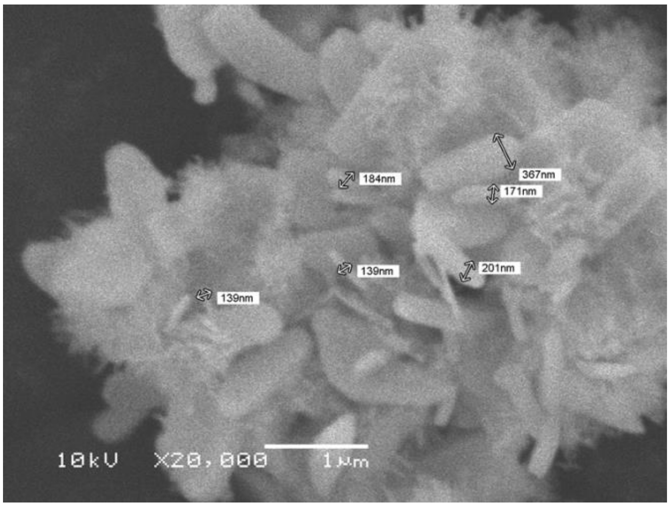

Figure 11. SEM image of [$NiHLCl_2(H_2O)_2$].

3.5. SEM Analysis.

SEM is the most advanced and commonly used method for characterizing the size, shape, arrangement and degree of agglomeration of nanoparticles. High-resolution images of the inspected compounds were given in Fig. 6. These images showed that the free ligand (HL) possesses a spherical like ball morphology on the micrometer scale. An abrupt change in its morphology was observed after the chelation of Cr(III), Mn(II), Fe(III), Co(II) and Ni(II) (Figs.7-11) to HL. The figures showed that Cr(III), Mn(II) and Fe(III) complexes had spherical particles on plates structures while Co(II) complex had very fine aggregates of needle, finally Ni(II) complex had a flower structure with small rods on the nanometer scale.

Table 3. Electronic spectral absorption bands of HL and its metal complexes and the ligand field parameter and magnetic moments of the complexes.

Compound	Band position, cm^{-1}	Assignment	Ligand field parameters			μ_{eff} (B.M.)
			D_q (cm^{-1})	B (cm^{-1})	β	
HL	35478, 32533 28573	$\pi \rightarrow \pi^*$ $n \rightarrow \pi^*$	-	-	-	-
[$CrHLCl_3(H_2O)$]	17778 20841	$^4A_{2g}(F) \rightarrow {}^4T_{2g}(F)$ $^4A_{2g}(F) \rightarrow {}^4T_{1g}(F)$	1633	441	0.654	3.78
[$MnLCl(H_2O)_3$]	16933 23695	$^6A_1 \rightarrow {}^4A_1(G)$ $^6A_1 \rightarrow {}^4T_1(D)$	878	802	0.81	5.89
[$FeLCl_2(H_2O)_2$]	22980 26778	$^6A_{1g} \rightarrow {}^4T_{2g}(G)$ $^6A_{1g} \rightarrow {}^4E_g$ (G)	742	674	0.75	5.98
[$CoHLCl_2(H_2O)_2$]	18251 19230 24140	$^4A_2 \rightarrow {}^4T_1(P)$ $^4A_2 \rightarrow {}^4T_1(F)$ LMCT	926	965	0.89	3.55
[$NiHLCl_2(H_2O)_2$]	17106 21830	$^3A_{2g} \rightarrow {}^1T_{1g}(P)$ $^3A_{2g} \rightarrow {}^3T_{1g}(F)$	938	959	0.89	2.79

LMCT: ligand to metal charge transfer.

Table 4. The molecular parameters of HL and its metal complexes.

Compound	Total Energy (kcal/mol)	Binding Energy (kcal/mol)	Dipole moment (debye)	Electronic Energy (kcal/mol)	Heat of Formation (kcal/mol)	HOMO (eV)	LUMO (eV)
1	-51509	-2868	5.784	-314888	87.74	-8.766	-1.059
2	-86827	-3468	8.411	-580224	-166.22	-5.125	-0.884
3	-89995	-3671	3.116	-605125	-178.87	-4.172	-0.138
4	-93150	-3722	1.789	-620579	-332.92	-5.194	-1.010
5	-99481	-3820	4.312	-648393	-375.69	-4.436	-1.143
6	-105260	-3733	3.000	-648430	-288.47	-8.811	-0.836

4. CONCLUSIONS

The present manuscript deals with the green syntheses, spectral characterizations, theoretical calculations of HL and its Cr(III), Mn(II), Fe(III), Co(II) and Ni(II) complexes. All these characterization studies conclude the synthesis of HL and its chelation with Cr(III), Mn(II), Fe(III), Co(II) and Ni(II). All the reported Cr(III), Mn(II), Fe(III), Co(II) and Ni(II) complexes are octahedral in nature. The bonding of the primary ligand within all complexes takes place through azomethine nitrogen atoms and thione sulphur atoms. Furthermore, investigations on the crystal structures of HL and its Cr(III), Mn(II), Fe(III), Co(II) and Ni(II) complexes will be carried out to achieve a better understanding of the structural properties. SEM images showed that the free ligand (HL) possesses a spherical like ball morphology on the micrometer scale. An abrupt change in its morphology was observed after the chelation of Cr(III), Mn(II), Fe(III), Co(II) and Ni(II) to HL. The figures showed that Cr(III), Mn(II) and Fe(III) complexes had spherical particles on plates structures while co(II) complex had very fine aggregates of needle, finally Ni(II) complex had a flower structure with small rods on the nanometer scale.

5. REFERENCES

1. Kaupp, G.; Naimi-Jamal, M.R.; Ren, H.; Zoz, H.; in eds.: Cao, G.; Delogu, F.; Orru, R. In: *Advanced Technologies Based on Self-Propagating and Mechanochemical Reactions for Environmental Protection; Research Signpost: Kerala, India* **2003**, 83-100.
2. Ren, H.; Zoz, G.; Kaupp, G.; Naimi-Jamal, M.R. Environmentally Protecting Reactive Milling. In: *Advances in Powder Metallurgy & Particulate Materials*, 2003; 216-222.
3. Zoz, H.; Kaupp, G.; Ren, H.; Goepel, K.; Naimi-Jamal, M.R. Recycling of EAF dust by semi-continuous high kinetic processing. *Metall.* **2005**, *59*, 293-296.
4. Bakhshai, A.; Pragani, R.; Takacs, L. Self-propagating reaction induced by ball milling in a mixture of Cu2O and Al powders. *Metall. Mater. Trans.* **2002**, *33*, 3521-3526, http://dx.doi.org/10.1007/s11661-002-0339-3.
5. Al-Noaimi, M.Z.; Saadeh, H.; Haddad, S.F.; El-Barghouthi, M.I.; El-Khateeb, M.; Crutchley, R.J. Syntheses, crystallography and spectroelectrochemical studies of ruthenium azomethine complexes, *Polyhedron* **2007**, *26*, 3675-3685. https://doi/org/10.1016/j.poly.2007.03.045.
6. Smith, J.W.; Patai, S. The chemistry of the Carbon-Nitrogen Double Bond. *Interscience* **1970**.
7. Ishak, N.N.M.; Jamsari, J.; Ismail, A.Z.; Tahir, M.I.M.; Tiekink, E.R.T.; Veerakumarasivam, A.; Ravoof, T.B.S.A. Synthesis, characterisation and biological studies of mixed-ligand nickel (II) complexes containing imidazole derivatives and thiosemicarbazide Schiff bases. *Journal of Molecular Structure* **2019**, *1198*, http://dx.doi.org/10.1016/j.molstruc.2019.126888.
8. Yousef, T.A.; Abu El-Reash, G.M.; El-Gamal, O.; Sharaa, B.M.; Ligational, DFT, optical band gap and biological studies on Mn(II), Co(II) and Ni(II) complexes of ethyl and allyl thiosemicarbazides ending by thiazole group. *Journal of Molecular Liquids* **2018**, *251*, 423–437, https://doi.org/10.1016/j.molliq.2017.12.022.
9. Eğlence-Bakır, S.; Sacan, O.B.; Şahin, M.C.; Yanardag, R.B.; Ülküseven, B. Dioxomolybdenum(VI) complexes with 3-methoxy salicylidene-N-alkyl substituted thiosemicarbazones. Synthesis, characterization, enzyme inhibition and antioxidant activity. *Journal of Molecular Structure* **2019**, *1194*, 35-41, https://doi.org/10.1016/j.molstruc.2019.05.077.
10. Yousef, T.A.; Abu El-Reash, G.M.; Abu AL-Zahab, M.; Safaan, M. A.A.; Physicochemical investigations, biological studies of the Cr(III), Mn(II),Fe(III), Co(II), Ni(II), Cu(II), Zn(II), Cd(II), Hg(II) and UO2(VI) complexes of picolinic acid hydrazide derivative: A combined experimental and computational approach. *Journal of Molecular Structure* **2019**, *1197*, 564-575, https://doi/org/10.1016/j.molstruc.2019.07.088.
11. Sreekanth, A.; Kala, U.L.; Nayar, C.R.; Kurup, M. R. P. Cobalt(III) complexes of 2-hydroxyacetophenone N(4)-phenyl semicarbazone containing heterocyclic coligands: syntheses, structure and spectral studies . *Polyhedron* **2004**, *23*, 41–47. https://doi.org/10.1016/j.poly.2003.09.029.
12. Yousef, T.A.; Al Duaij, O.K. Green Synthesis Approach For Thiosemicabazone Derivative Cu (II) Complexes With Elaborated Spectral, Theoretical Studies Research Journal of Pharmaceutical, Biological and Chemical Sciences 2019, 10, 1598-1611.
13. HyperChem Version 8.0, Hypercube, Inc., 2002
14. Allinger, N.L. Conformational analysis. 130. MM2. A hydrocarbon force field utilizing V1 and V2 torsional terms. *J. Am. Chem. Soc.* **1977**, *99*, 8127–8134 , https://doi.org/10.1021/ja00467a001.
15. Yousef, T.A.; Abu El-Reash, G.M.; El-Tabai, M.N.; Comparative studies on P-vanillin and O-vanillin of 2-hydrazinyl-2-oxo-N-phenylacetamide and their Mn(II) and Co(II) complexes. *Journal of Molecular Structure* 2018, 1159, 246-258, https://doi/org/10.1016/j.molstruc.2018.01.003.
16. Yousef, T.A.; Abu El-Reash, G.M.; Al-Jahdali, M.; El-Bastawesy, R.E.R. Synthesis, spectral characterization and biological evaluation of Mn(II), Co(II), Ni(II), Cu(II), Zn(II) and Cd(II) complexes with thiosemicarbazone ending by pyrazole and pyridyl rings. *Spectrochimica Acta Part A: Molecular and Biomolecular Spectroscopy* **2014**, *129*, 163–172, https://doi.org/10.1016/j.saa.2014.02.184.
17. Yousef, T.A.; El-Gammal, O.A.; Ghazy, S.E.; et al. Synthesis, spectroscopic characterization, pH-metric and thermal behavior on Co(II) complexes formed with 4-(2-pyridyl)-3-thiosemicarbazide derivatives. *Journal of Molecular Structure* **2011**, *1004*, 271–283, https://doi.org/10.1016/j.molstruc.2011.08.020.
18. Yousef, T.A.; Abu El-Reash, G.M.; El-Rakhawy, E.R. Structural, spectral, thermal and biological studies on (E)-2-(1-(4-hydroxyphenyl)ethylidene)-N-(pyridin-2-yl(hydrazinecarbothioamide and its metal complexes. *Spectrochimica Acta Part A: Molecular and Biomolecular Spectroscopy* **2014**, *133*, 568–578, https://doi.org/10.1016/j.saa.2014.05.041.
19. Bedier, R.A.; Yousef, T.A.; Abu El-Reash, G.M.; El-Gammal, O.A. Synthesis, structural, optical band gap and biological studies on iron(III), nickel (II), zinc (II) and mercury (II) complexes of benzyl amonoxime pyridyl thiosemicarbazone. *Journal of Molecular Structure* **2017**, *1139*, 436-446, http://dx.doi.org/10.1016%2Fj.molstruc.2017.03.054.
20. Yousef, T.A.; Abu El-Reash, G.M.; El-Gammal, O.A.; Bedier, R.A. Synthesis, characterization, optical band gap, in vitro antimicrobial activity and DNA cleavage studies of some metal complexes of pyridyl thiosemicarbazone. *Journal of Molecular Structure* **2013**, *1035*, 307–317, https://doi.org/10.1016/j.molstruc.2012.10.058.
21. Zaky, R.R.; Yousef, T.A. Spectral, magnetic, thermal, molecular modelling, ESR studies and antimicrobial activity of (E)-3-(2-(2-hydroxybenzylidene)hydrazinyl -(3-oxo-n(thiazole-2-yl)propanamide complexes. *Journal of Molecular Structure* **2011**, *1002*, 76-85, http://dx.doi.org/10.1016/j.molstruc.2011.06.050.

22. Zaky, R.R.; Yousef, T.A.; Ibrahim, K.M. Co(II), Cd(II), Hg(II) and U(VI)O_2 complexes of o-hydroxyacetophenone[N-(3-hydroxy-2-naphthoyl)] hydrazone :Physicochemical study, thermal studies and antimicrobial activity. *Spectrochimica Acta Part A: Molecular and Biomolecular Spectroscopy* **2012**, *97*, 683–694, https://doi.org/10.1016/j.saa.2012.05.086.

23. Bayer, E.; Witte, C.G. The coordination chemistry of cis- and trans-1, 2-bis(2-pyridyl)ethylene. four-, five-, and six-coordinate complexes of nickel(ii) and zinc(h). *Journal of coordination chemistry* **1977**, *7*, 13, https://doi.org/10.1080/00958977708073032.

24. Yousef, T.A.; El-Gammal, O.A.; Ahmed, S.F.; Abu El-Reash, G.M. Structural, DFT and biological studies on Co(II) complexes of semi and thiosemicarbazide ligands derived from diketo hydrazide. *Journal of Molecular Structure* **2014**, *1076*, 227–237, https://doi.org/10.1016/j.molstruc.2014.07.053.

25. Yousef, T.A.; Abu El-Reash, G.M.; El-Tabai, M.N. Comparative studies on P-vanillin and O-vanillin of 2-hydrazinyl-2- oxo-N-phenylacetamide and their Mn(II) and Co(II) complexes. *Journal of Molecular Structure* **2018**, *1159*, 246-258, https://doi.org/10.1016/j.molstruc.2018.01.003.

26. Yousef, T.A.; Alduaij, O.K.; Ahmed, S.F.; Abu El-Reash, G.M.; El-Gammal, O.A. Structural, DFT and biological studies on Cr(III) complexes of semi and thiosemicarbazide ligands derived from diketo hydrazide. *Journal of Molecular Structure* **2016**, *1125*, 788-799, https://doi.org/10.1016/j.molstruc.2016.07.045.

27. Yousef, T.A.; Abu El-Reash, G.M.; El Morshedy, R.M. Quantum chemical calculations, experimental investigations and DNA studies on (E)-2-((3-hydroxynaphthalen-2-yl)methylene)-N-(pyridin-2-yl) hydrazinecarbothioamide and its Mn(II), Ni(II), Cu(II), Zn(II) and Cd(II) complexes. *Polyhedron* **2012**, *45*, 71–85, https://doi.org/10.1016/j.poly.2012.07.041.

28. Yousef, T.A.; Abu El-Reash, G.M.; El Morshedy, R.M. Structural, spectral analysis and DNA studies of heterocyclic thiosemicarbazone ligand and its Cr(III), Fe(III) ,Co(II) Hg(II), and U(VI) complexes. *Journal of Molecular Structure* **2013**, *1045*, 145–159, https://doi.org/10.1016/j.molstruc.2013.03.060.

29. Yousef, T.A.; Alduaij, O.K.; Abu El-Reash, G.M.; El Morshedy, R.M. Semiempirical studies, spectral analysis, in vitro antibacterial and DNA degradation studies of heterocyclic thiosemicarbazone ligand and its metal complexes. *Journal of Molecular Liquid* **2016**, *222*, 762–776, https://doi.org/10.1016/j.molliq.2016.07.075.

30. Yousef, T.A.; Abu El-Reash, G.M.; Synthesis, and biological evaluation of complexes based on thiosemicarbazone ligand *Journal of Molecular Structure* ***2020**, 2021*, https://doi.org/10.1016/j.molstruc.2019.127180

Yousef, T.A.; Abu El-Reash, G.M.; El-Gammal, O.A.; Ahmed S.F. Structural, DFT and biological studies on Cu(II) complexes of semi and thiosemicarbazide ligands derived from diketo hydrazide. *Polyhedron* **2014**, *81*, 749–763, https://doi.org/10.1016/j.poly.2014.07.035.